Journal of Sound and Vibration (2000) **235**(3), 375–403
doi:10.1006/jsvi.1999.2927, available online at http://www.idealibrary.com on IDEAL®

DAMPING IDENTIFICATION IN MULTI-DEGREE-OF-FREEDOM SYSTEM VIA A WAVELET-LOGARITHMIC DECREMENT—PART 2: STUDY OF A CIVIL ENGINEERING BUILDING

S. Hans, E. Ibraim, S. Pernot, C. Boutin and C.-H. Lamarque

Ecole Nationale des Travaux Publics de l'Etat, DGCB/LGM, URA CNRS 1652, 1 *rue Maurice Audin, F* 69 518 *Vaulx-en-Velin, Cedex, France*

(*Received* 25 *June* 1998, *and in final form* 8 *November* 1999)

In a previous paper entitled "Damping identification in multi-degree-of-freedom (m.d.o.f.) systems via wavelet-logarithmic decrement—Part 1: theory", a wavelet-logarithmic decrement formula was established to estimate damping in multi-degree-of-freedom systems from time-domain responses. Numerical validation was then investigated using the dynamic response of exact single-degree-of-freedom systems that were artificially perturbed with a Gaussian noise. Part 2 is now dedicated to the application of the wavelet procedure to identify the damping of *in situ* dynamic responses of a civil engineering building excited with both harmonic and shock testings.

1. INTRODUCTION

Until recently, the complex question of vulnerability of existing civil engineering buildings has been mainly treated using qualitative approach based on post-earthquake observations [1]. On the other hand, experimental studies are essentially devoted to the design of new structures. The present work refers to more general studies [2–4] whose goal is to contribute to give a quantitative estimation of seismic vulnerability and guideline for retrofitting of civil engineering buildings using an experimental approach. Experimental data are borrowed from vibrational testing campaigns related to recent buildings (1955–1975) which concern nearly 30% of the population in France. When analyzing the dynamic response of structures the parameters of fundamental engineering importance are the natural frequencies of vibration and the damping ratio bound to the eigenmodes. Damping identification of multimodal response also appears to be of crucial interest. The aim of the study is to apply the wavelet-logarithmic decrement established in reference [5] to estimate the non-dimensional damping ratio of the first two flexural modes of a civil engineering building (in both longitudinal and transverse directions) from experimental time responses.

The paper is organized as follows: Section 2 describes the experimental procedure including the instrumentation, the testing procedures and a detailed description of the tested civil engineering building. In Section 3, the experimental results are introduced and a few comments are outlined. In Section 4, the wavelet-logarithmic decrement procedure is applied to estimate the non-dimensional damping ratio of the fundamental and the first harmonic bending mode in both the longitudinal and transverse directions, according to

0022-460X/00/330375 + 29 $35.00/0

harmonic/shock test responses. Some conclusions are then drawn as for the efficiency of the proposed method.

2. THE EXPERIMENTAL PROCEDURE

2.1. INSTRUMENTATION

Three different types of excitations were used to measure frequencies, mode shapes and non-dimensional damping ratios:

- Ambient vibration excitation mainly produced by traffic and wind.
- Harmonic excitation applied at the top level with a small mechanical shaker constituted by two counter-rotating masses.
- Shock excitation on the structure induced by a mechanical shovel.

Whatever the excitation source is, acceleration amplitudes are assumed to be small enough not to move the structure's behavior outside its elastic domain. Moreover, the building response is recorded with a four-channel accelerometer–recorder system composed of

- Four unidirectional piezometric accelerometers depicted in Figure 1(a) characterized by an excellent linearity in the frequency width of 0–8 kHz and a sensibility of 0·05 mm s^{-2} equivalent to 5×10^{-6} g.

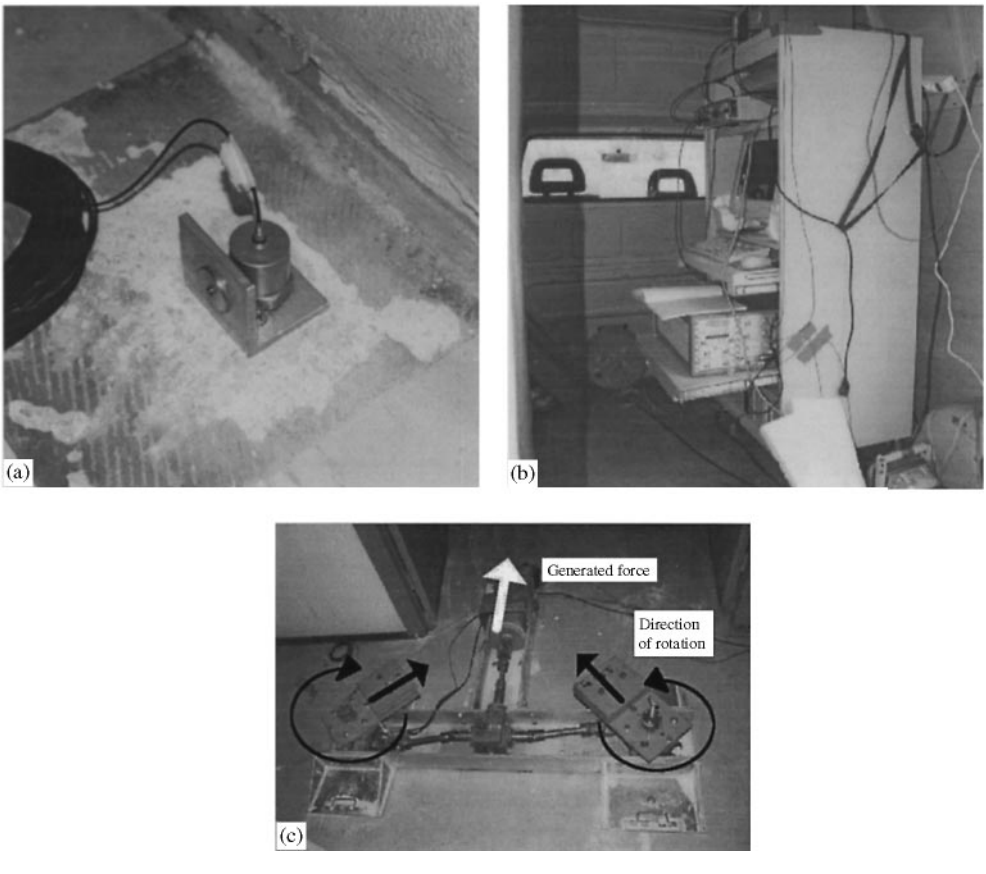

Figure 1. Building instrumentation. (a) Accelerometer in vertical position. (b) Acquisition system. (c) Harmonic shaker.

- A four-channel HP3566/67 recorder system featuring a synchronized analogical acquisition of signal response.
- A PC equipped with the HP software "Paragon" driving the hardware storage and the signal processing as displayed in Figure 1(b).

A sampling frequency of 128 Hz and a time-recording of 64 s were retained to avoid problems of spectrum folding and cut-off frequency, permitting to analyze a 0–50 Hz frequency bandwidth sufficient to capture the vibration modes of interest.

2.2. TESTED BUILDING

The tested structure was a regular eight-story building made in 1970 and depicted in Figures 2(a) and 2(b). Shear walls are made in concrete and floors in reinforced concrete.

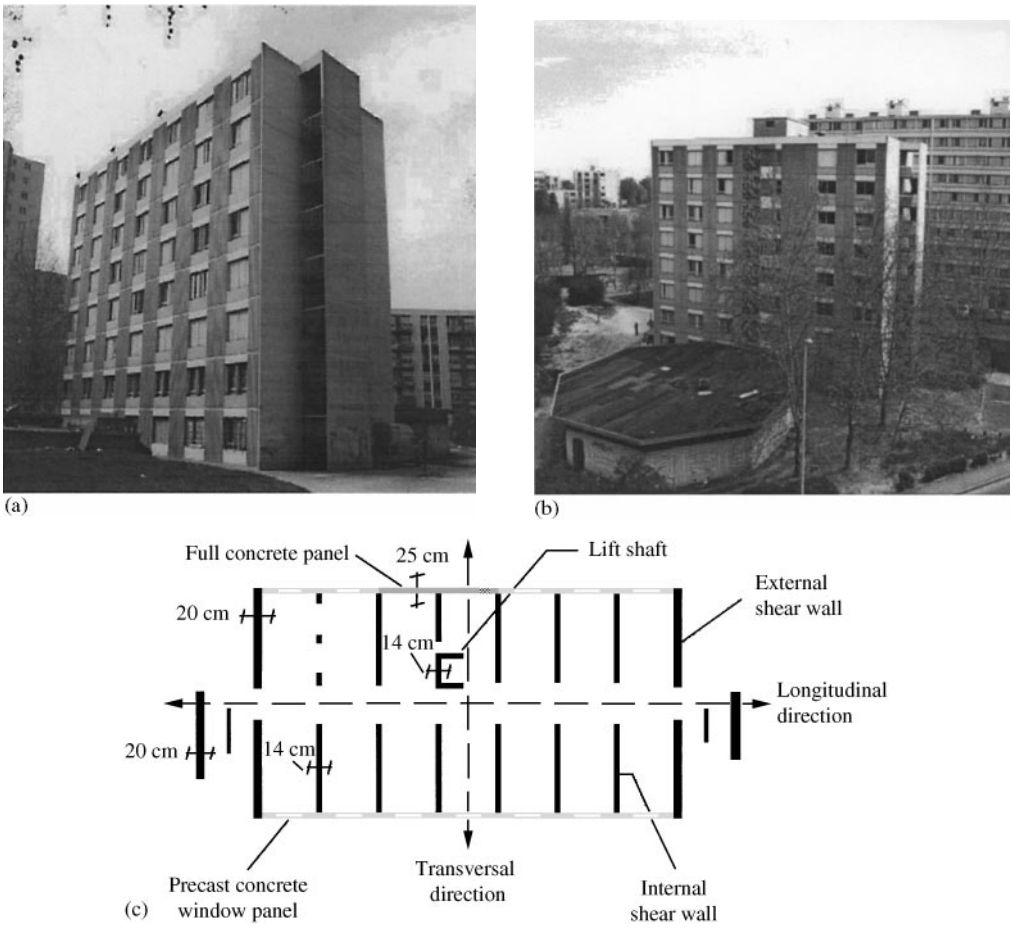

Figure 2. The tested seven-level building (1970). Height: 22 m. Length: 30 m. Width: 14 m. (a) South front. (b) North front. (c) Typical floor plan showing: Shear walls in concrete, internal: 0·14 m × 6 m × 2·55 m, external: 0·20 m × 6 m × 2·55 m. Precast concrete window panels, 0·20 m × 4 m × 2·55 m. Window: 2·10 m × 1·53 m. Two full concrete façade panels, 0·20 m × 4 m × 2·55 m. Lift shaft: 2 walls 0·14 m × 1·60 m × 2·55 m, 1 wall 0·14 m × 1·80 m × 2·55 m. Floors in reinforced concrete, thickness: 0·15 m.

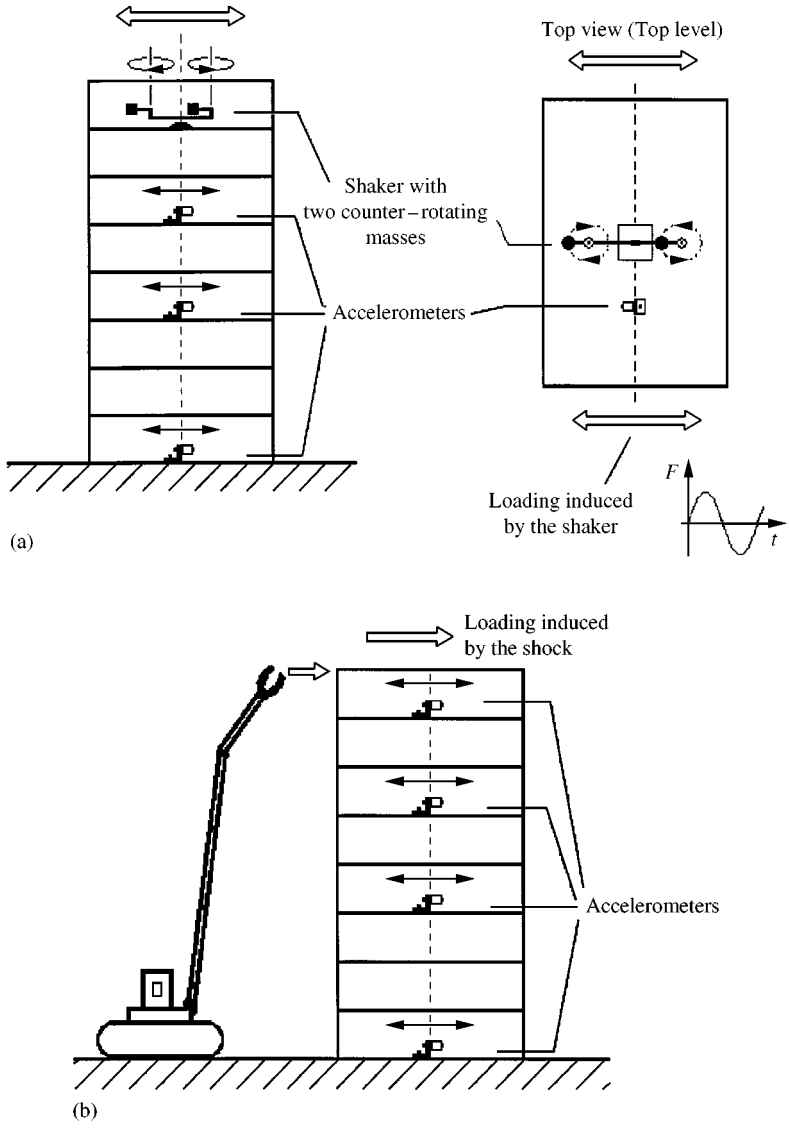

Figure 3. Vertical and horizontal disposal of accelerometers. (a) Harmonic test. (b) Shock test.

The dimensions of the building are 22 m high, 30 m long and 14 m wide. A general view of a typical floor map is introduced in Figure 2(c). The longitudinal frontage is constituted of precast concrete window panels, connected to the main structure with steel angle clips.

2.3. TESTING PROCEDURES

The accelerometers are located in the center of the structural cross-section, one at the first floor, one at the top floor and the others in the intermediate levels. Longitudinal

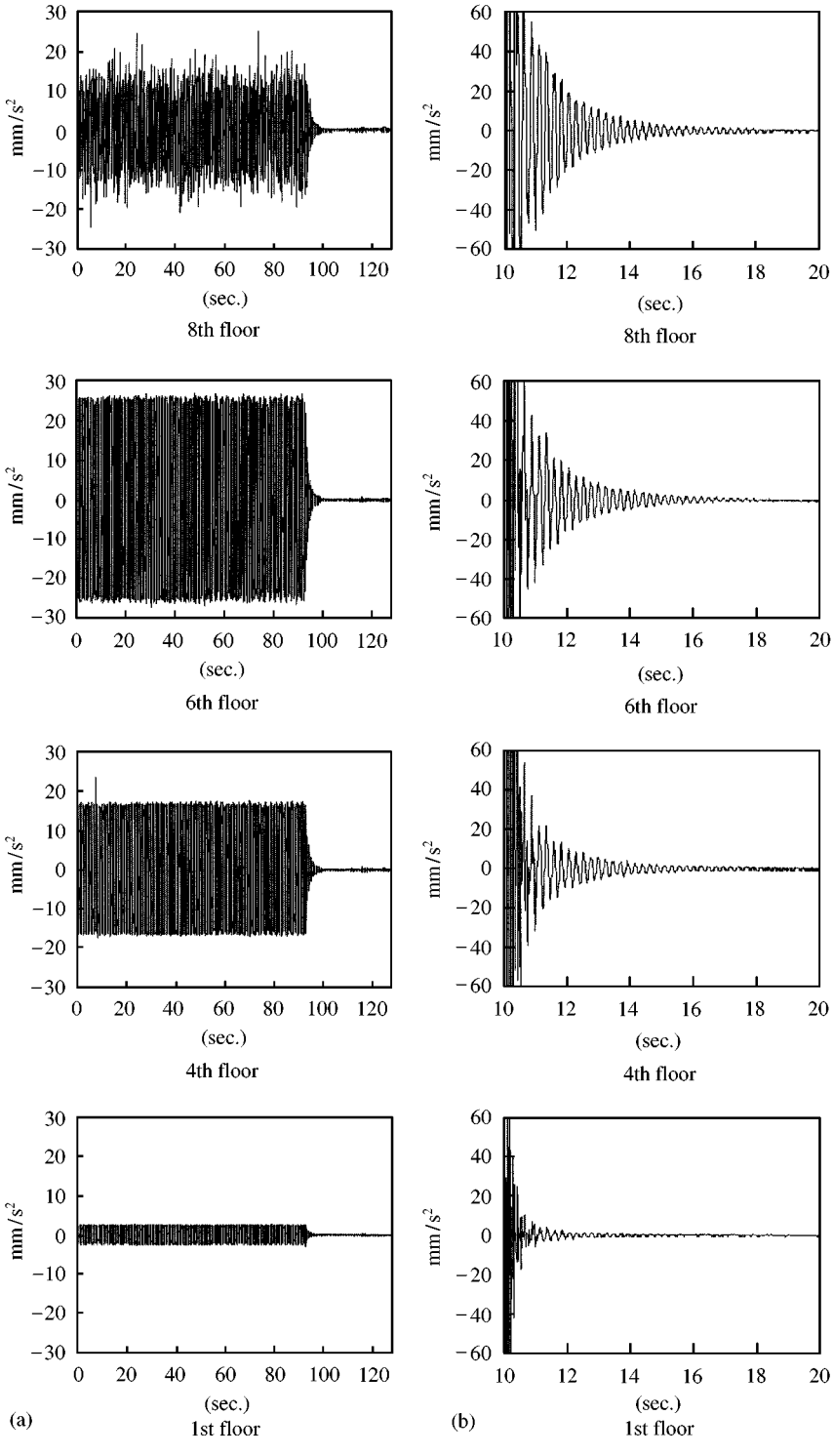

Figure 4. Time-response recordings of the building vibrations in the longitudinal direction with respect to (a) harmonic and (b) shock excitations.

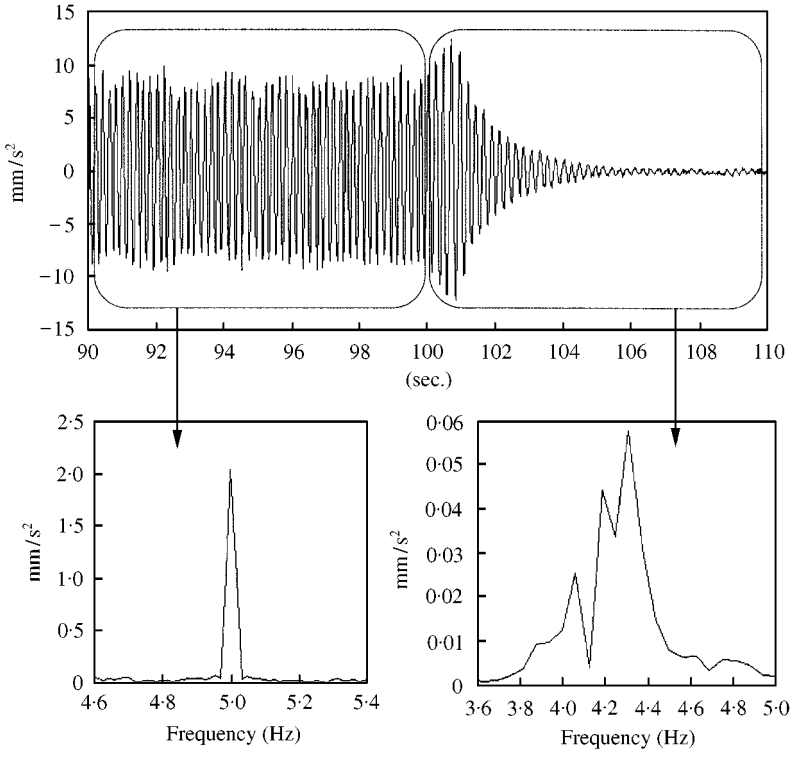

Figure 5. Frequency spectrum response in both steady state (5 Hz forcing) and free oscillations.

(lengthwise) or transverse (in the direction of the width) oscillations may independently be recorded when varying the accelerometers orientation. As floors are sufficiently stiff, accelerations recorded at the center of a level are representative of the entire floor, the validity of this assumption being experimentally checked.

2.3.1. *Ambient vibration test*

The ambient vibration test is a direct and practical method [6, 7] to determine modal parameters of structures. It is based upon measuring the response of structures to background noise due to wind, road circulation or any other human activity. These stochastic vibrations excite the building that selectively responds in its characteristic modes of oscillations. This testing procedure may easily be carried out and does not require shakers-induced forced vibrations. Generally speaking, experimental recordings witness a good repeatability and stability in the measurements. The order of magnitude of horizontal acceleration is approximately 10^{-5} g. This type of excitation is only used to calibrate the harmonic tests in the following study.

2.3.2. *Harmonic test*

A dynamic shaker [8] with two counter-rotating masses (see Figure 1(c)) is fixed at the top floor as displayed in Figure 3(a). It delivers a unidirectional force controlled in frequency (given by the angular velocity) and amplitude (varying with the square of frequency). The frequency range of excitation is limited between 1 and 7 Hz, and the

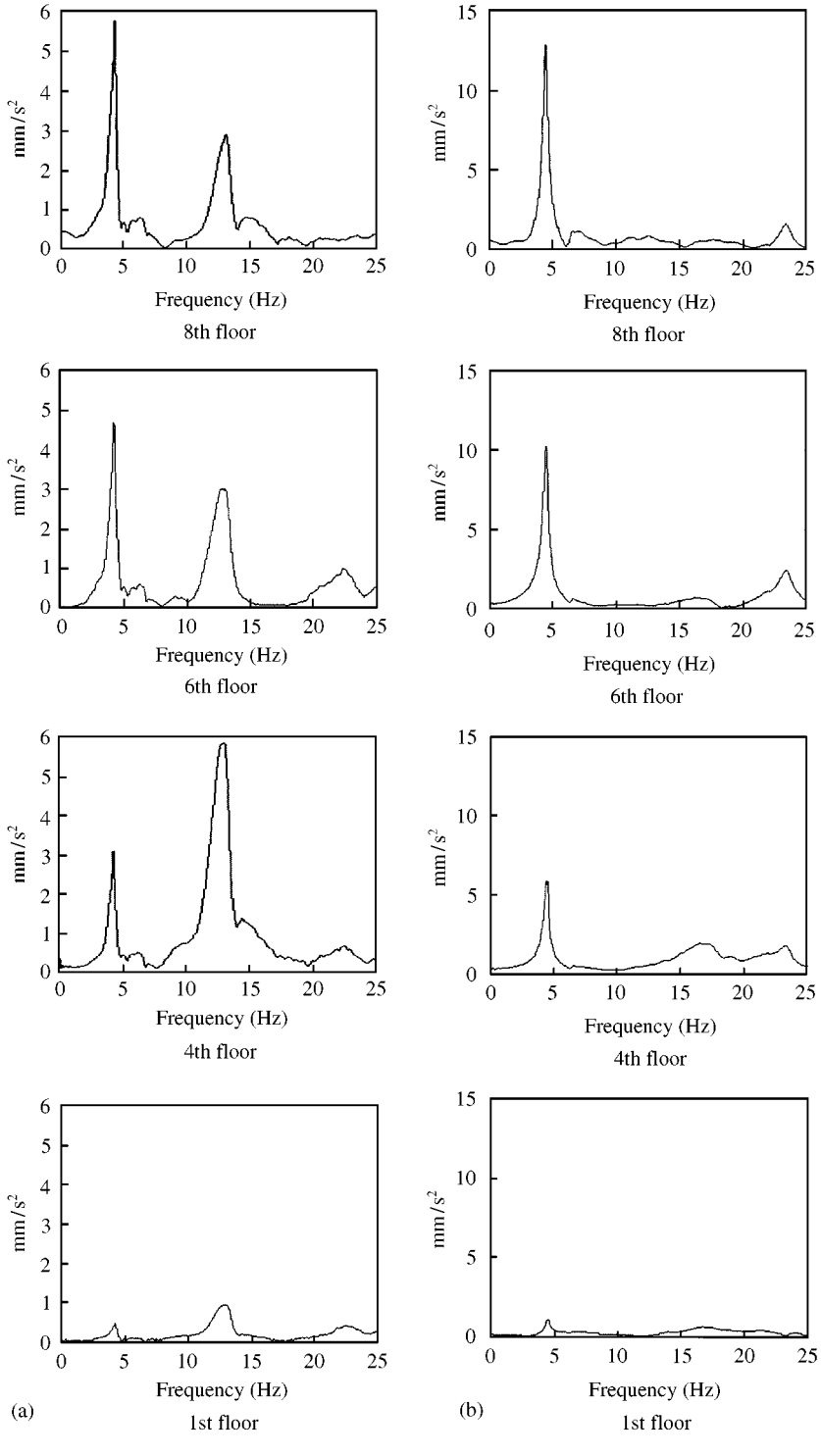

Figure 6. Spectrum response of the building excited with a head shock, respectively, in the (a) longitudinal and (b) transverse directions.

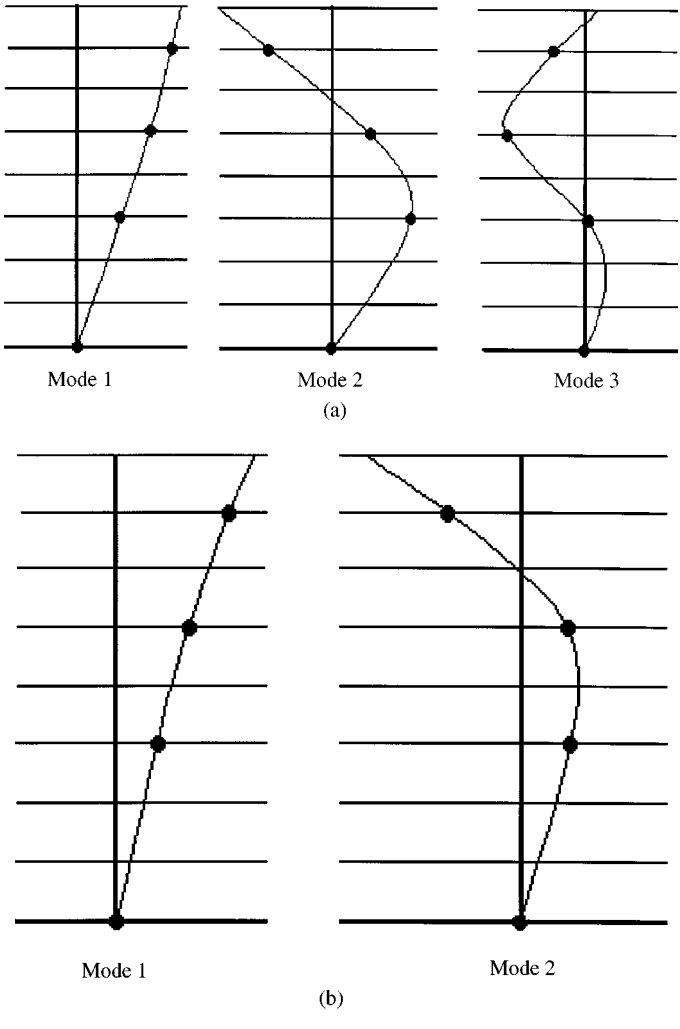

Figure 7. Mode shapes in a shock test configuration. (a) longitudinal mode shapes. (b) Transverse mode shapes.

TABLE 1

Shock test: *Frequency and non-dimensional damping of the first natural modes in both longitudinal and transverse directions*

	Mode 1	Mode 2	Mode 3
Eigenfrequency (Hz)	4·25	12·8	22·5
Longitudinal direction			
Non-dimensional damping ξ (%)	3·5	4	2·8
Eigenfrequency (Hz)	4·5	15·7	
Transverse direction			
Non-dimensional damping ξ (%)	3	5	

amplitude of force can reach 10 kN. We can investigate both forced vibrations (at various frequencies) and free vibrations (with initial displacement and velocity) after cancelling the excitation. During the forced vibrations rating, the acceleration level ($10^{-3}g$) is about 100 times higher than the one due to ambient noise. Similar testing campaigns were carried out in the field of earthquake engineering on several-story civil engineering buildings and may be found in references [9–11].

A spectrum analysis shows that the imposed and response frequencies are identical, with no harmonics or sub-harmonics oscillations appearing which are often the signature of non-linearities. This result is due to the weak level of excitations which is not sufficient either to damage the structure or to impose significant deformations to the soil. In the case of forced excitations, the testing procedure consists in experimentally obtaining the amplitude-exciting frequency response curve of the structure. The presence of a resonant peak in this curve allows one to determine a modal frequency and an associated damping ratio with the range width method. In the case of free oscillations, modal frequencies and associated dampings are given by a Fourier analysis. In the presence of a single eigenmode, the associated damping is estimated from the time response using a standard logarithmic decrement procedure including a wavelet pre-filtering.

2.3.3. *Shock test*

Shocks on the structure were applied using a mechanical shovel. The impacts (not quantified) were achieved with the pliers of the mechanical shovel in the middle of the highest level of the building as displayed in Figure 3(b), in both the longitudinal and transverse directions. The maximum of acceleration ($10^{-2}g$) is, respectively, 1000 times and 10 times higher than the ambient noise or the harmonic excitation acceleration level. A Fourier analysis of signals permitted to locate precisely the eigenfrequency modes and rough damping estimates were obtained using the frequency bandwidth.

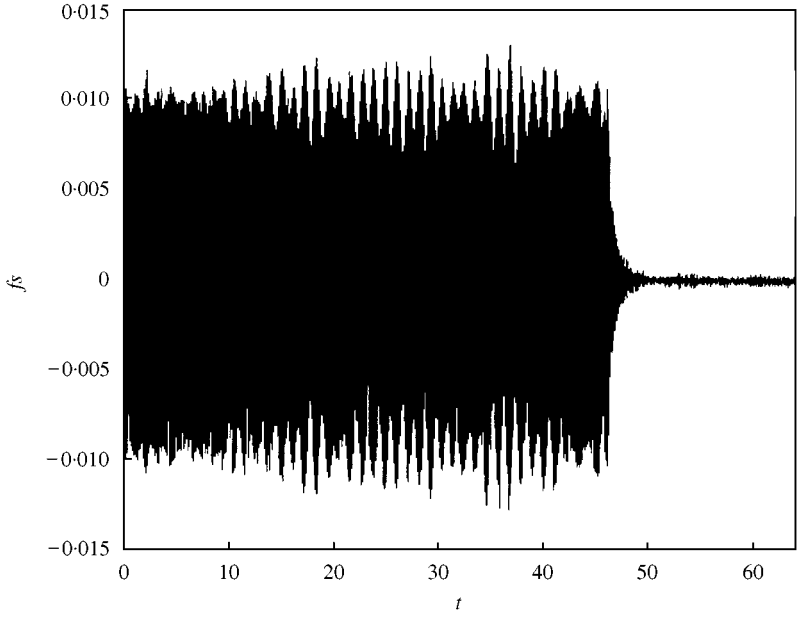

Figure 8. 6th floor original time-response to harmonic test (forced and free oscillations, longitudinal direction).

3. EXPERIMENTAL RESULTS

Experimental results are introduced according to the harmonic (free vibrations) and shock testing procedures.

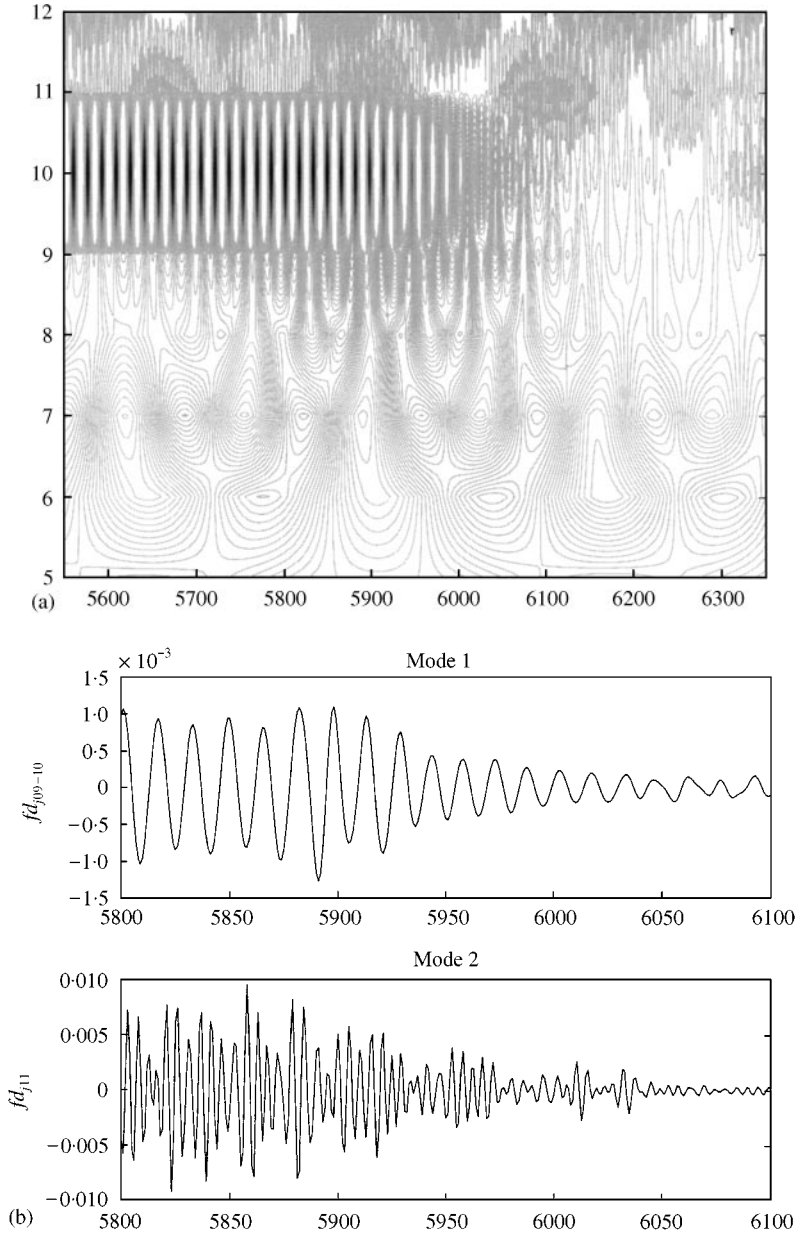

Figure 9. 6th floor longitudinal time-response to harmonic test (forced and free oscillations). (a) Wavelet pyramidal decomposition in terms of translation parameters k and scales J. (b) Reconstruction of the first (scales $J = 9, 10$) and second (scale $J = 11$) modal responses. (c) Detail channels $(fd_J)_{J=5,\ldots,12}$. (d) Approximation channels $(fs_J)_{J=5,\ldots,13}$.

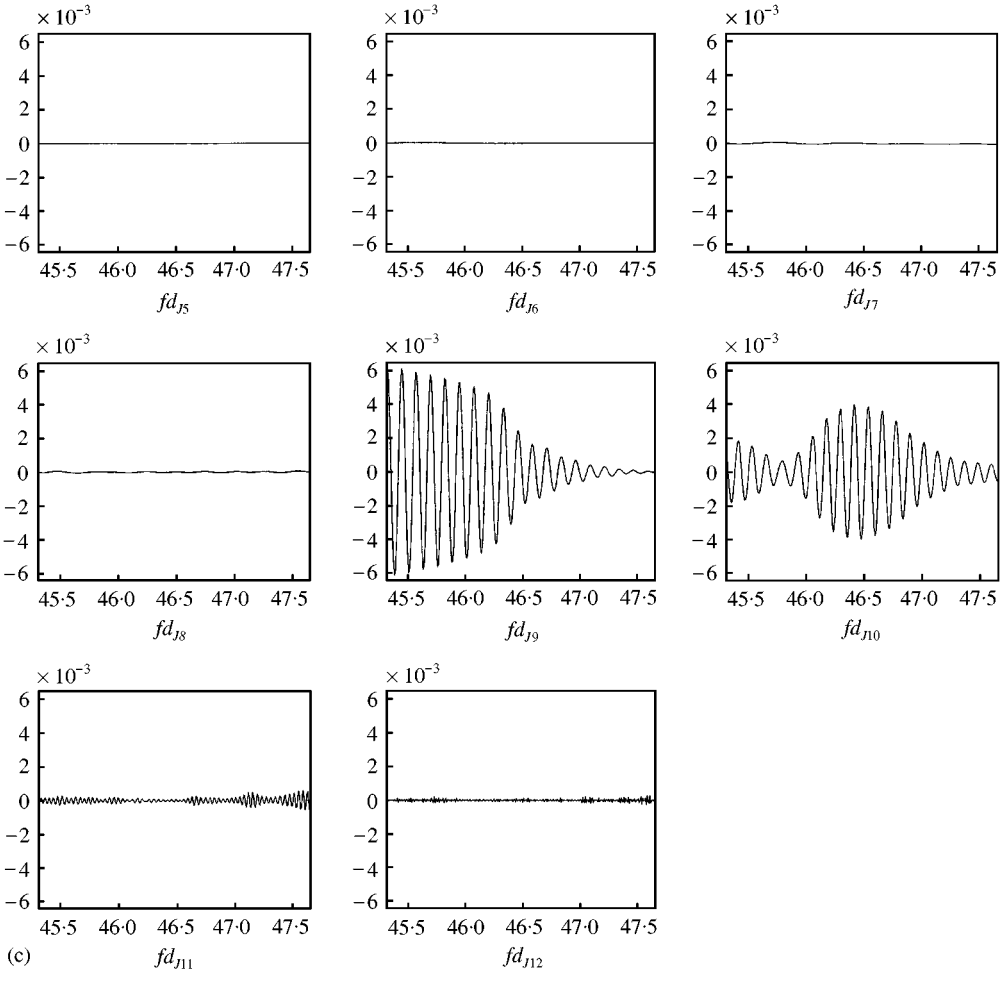

Figure 9. Continued.

3.1. MEASURES WITH A HARMONIC EXCITATION

Focusing on the free oscillations, a transient state is established before the structure reaches a steady state as displayed in Figure 4(a) illustrating the structure time response according to the different floors. Harmonic tests have been carried out with an exciting frequency ranging in the neighborhood of the first longitudinal and transverse modes, respectively, between 3·8 and 5 Hz for longitudinal modes and between 4 and 5 Hz for transverse modes. The frequency analysis depicted in Figure 5 shows that after cancelling the harmonic forcing, the building is no longer vibrating near the forcing frequency (steady state) but mostly near the fundamental mode located, respectively, at 4·21 and 4·58 Hz according to the longitudinal and transverse directions. Using a standard logarithmic-decrement the associated damping estimates are roughly $0{\cdot}028 \pm 0{\cdot}001$ and $0{\cdot}033 \pm 0{\cdot}004$. Several time-response perturbations noticed in Figure 4(a) (8th floor) are imputable to a very near proximity between the shaker and the 8th floor sensor.

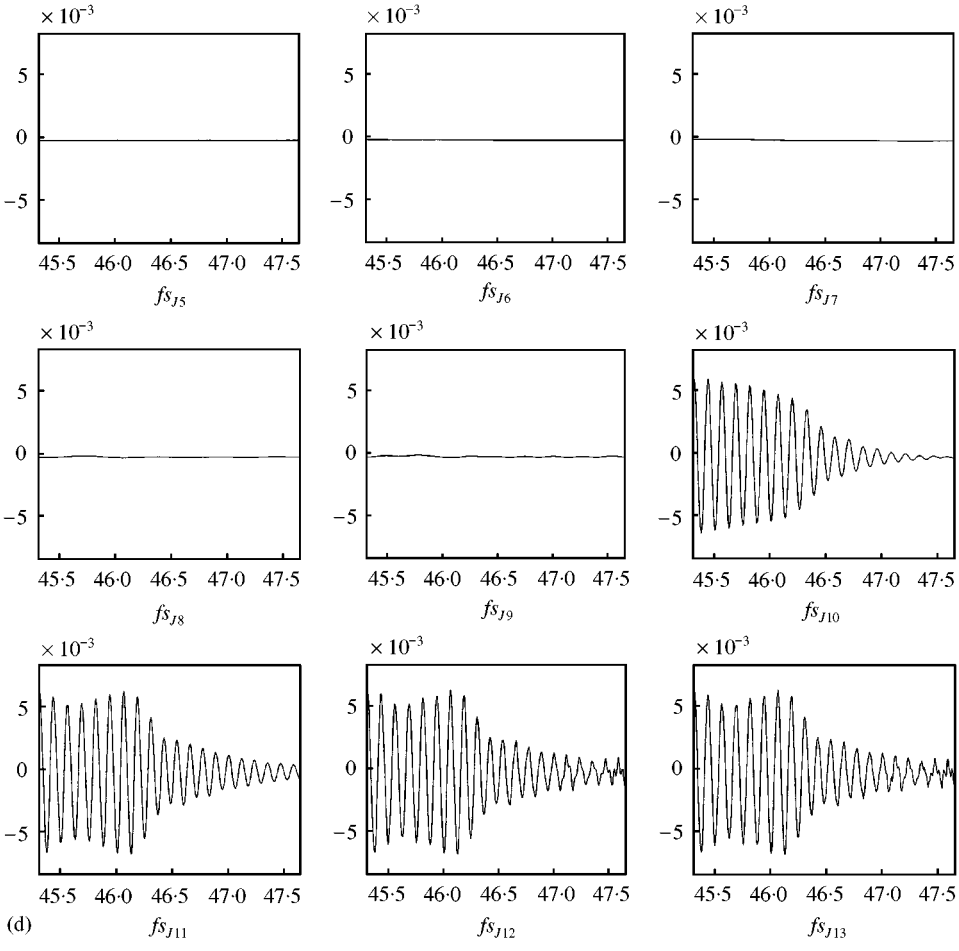

Figure 9. Continued.

3.2. MEASURES WITH A SHOCK EXCITATION

Shock tests highlight, respectively, three bending modes (4·24, 12·8, 22·5 Hz) in the longitudinal direction and two bending modes (4·5, 15·8 Hz) in the transverse direction as depicted in Figures 6(a) and 6(b). Spectrum responses permitted straightforwardly to draw the associated longitudinal and transverse mode shapes displayed in Figures 7(a) and 7(b). The frequency bandwidth drop method exhibits weakly accurate non-dimensional damping estimates ranging between 0·03 and 0·05 and gathered in Table 1. Though the damping estimate bound to the first mode is relevant, damping identification of the higher modes and their related error uncertainty appears to be critical.

3.3. CONCLUSION

Though the acceleration level ranges between $10^{-3}g$ and $10^{-2}g$ for a shock test (to be compared with levels of $10^{-4}g$ or $10^{-3}g$ in the case of free oscillations) the shock procedure

is more efficient and much easily carried out than its harmonic counterpart. It also provides a complete analysis of the dynamic behavior without damaging the structure. Therefore, it should be pointed out that both harmonic or shock excitation tests allow a good understanding of the whole structure's behavior also taking into account the contribution of the soil foundations. Both procedures accurately emphasize the first and the second eigenmodes of the building in longitudinal/transverse directions. Damping estimates are nevertheless too dispersive and specific analyses are required to refine forecasts.

4. APPLICATION OF THE WAVELET-LOGARITHMIC DECREMENT TO IDENTIFY DAMPING FEATURES OF THE TESTED BUILDING

The wavelet-logarithmic decrement formula (1) given by

$$c_i \simeq \frac{2^J}{k-l} \ln \left| \frac{O_{2^{ja}l}\left(f - f_\omega - \sum_{j=1}^{j=i-1} f_{\omega_j}\right)}{O_{2^{ja}k}\left(f - f_\omega - \sum_{j=1}^{j=i-1} f_{\omega_j}\right)} \right|, \quad 1 \leqslant i \leqslant N-1 \tag{1}$$

was theoretically established in reference [5] in the frame of a wavelet superabundant analysis to identify the damping ratio c_i related to the ith eigenfrequency mode in a multi-modal signal response. Similarly, the non-dimensional damping ξ_i related to the ith component response of a system of N oscillators given in the modal basis by

$$\ddot{q}_i + 2\xi_i\omega_i\dot{q}_i + \omega_i^2 q_i = f_i(t), \quad 1 \leqslant i \leqslant N \tag{2}$$

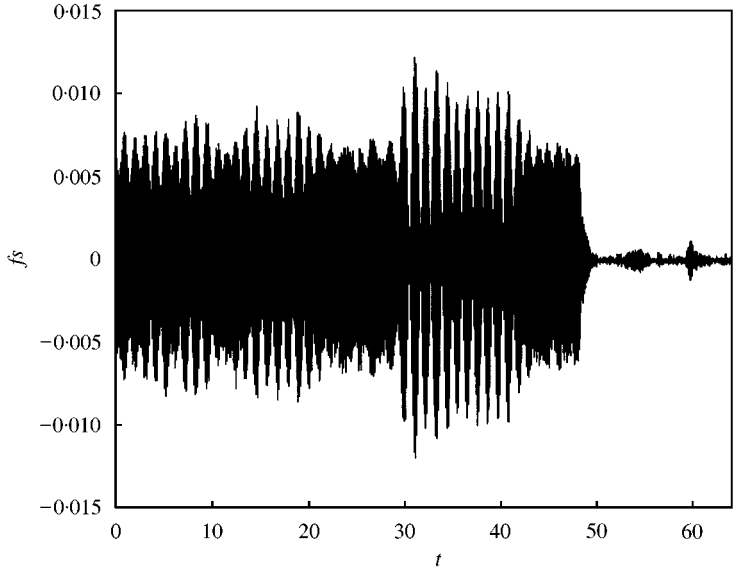

Figure 10. 6th floor original time-response to harmonic test (forced and free oscillations, transverse direction).

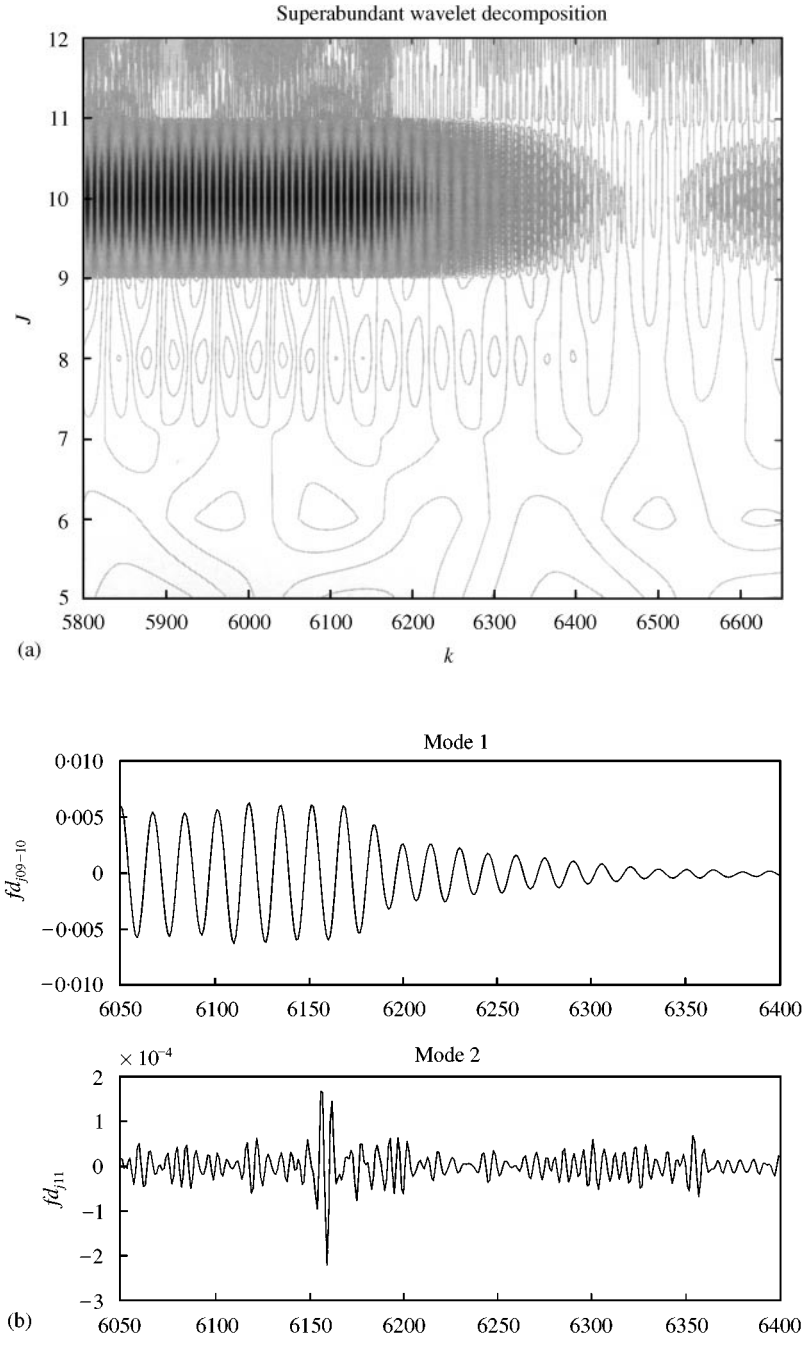

Figure 11. 6th floor transverse time-response to harmonic test (forced and free oscillations). (a) Wavelet pyramidal decomposition in terms of translation parameters k and scales J. (b) Reconstruction of the first (scales $J = 9, 10$) and second (scale $J = 11$) modal responses. (c) Detail channels $(fd_J)_{J=5,\ldots,12}$. (d) Approximation channels $(fs_J)_{J=5,\ldots,13}$.

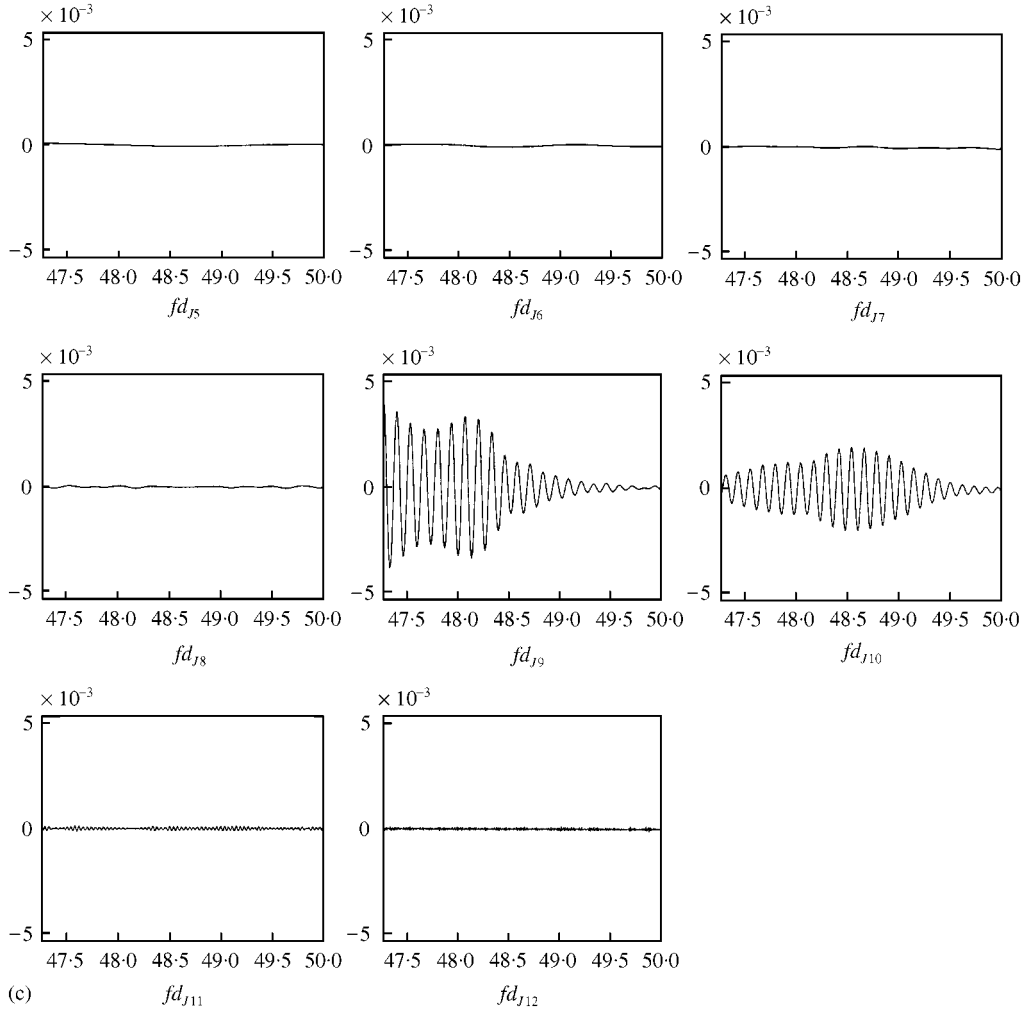

Figure 11. Continued.

is directly derived from equation (1) using the formula

$$\xi_i = \frac{\delta_i}{\sqrt{4\pi^2 + \delta_i^2}} \quad \text{with } \delta_i \simeq \ln \left| \frac{O_{2^{j_a}l}\left(f - f_\omega - \sum_{j=1}^{j=i-1} f_{\omega_j}\right)}{O_{2^{j_a}k}\left(f - f_\omega - \sum_{j=1}^{j=i-1} f_{\omega_j}\right)} \right|, \quad 1 \leqslant i \leqslant N-1 \tag{3}$$

As the key point relies on choosing an accurate analyzing scale j_a that will permit one to isolate eigenfrequency modes in the signal response, thorough explanations are given in the next section and a few harmonic/shock test responses are analyzed to illustrate the signal processing procedure.

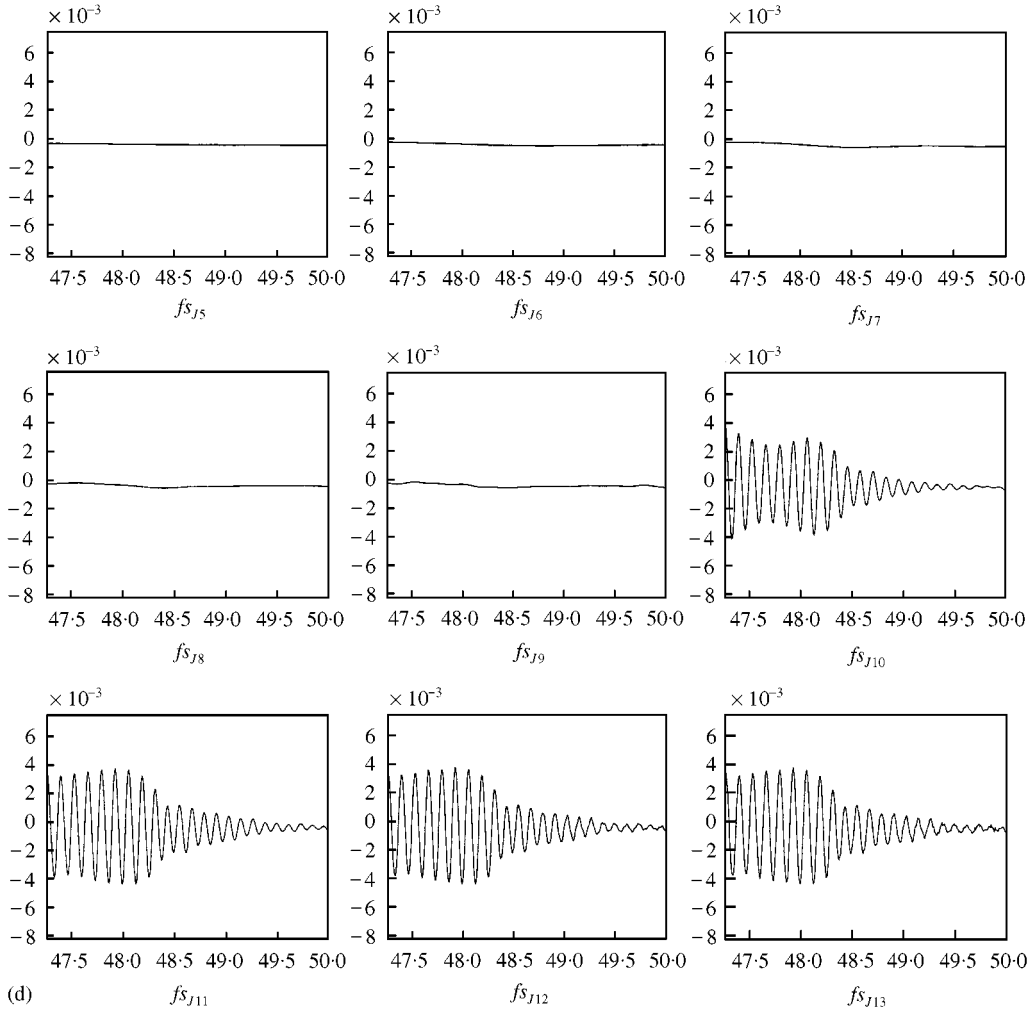

Figure 11. Continued.

4.1. SIGNAL PROCESSING PROCEDURE

Periodic spline wavelet tools have been implemented and gathered in a C++ library (http://www.entpe.fr) to process time-response signals and determine dynamic properties of the tested building. These tools provide efficient computations of wavelet/scaling coefficients of a signal and low-pass/band-pass signal filtering using wavelet pyramidal decomposition/reconstruction schemes. The library also includes superabundant features involved within the wavelet-logarithmic formula (1) permitting a better localization of superabundant wavelet coefficients extrema [5].

As soon as original time responses (Figures 8, 10, 12 and 14) have been recorded at the instrumented levels of the building and with respect to harmonic or shock excitations, in both the longitudinal and transverse directions, signals are processed using the wavelet library. Wavelet pyramidal decompositions mapping such as the ones displayed in Figures 9(a), 11(a), 13(a) and 15(a) are used to identify which detail components are bound to the

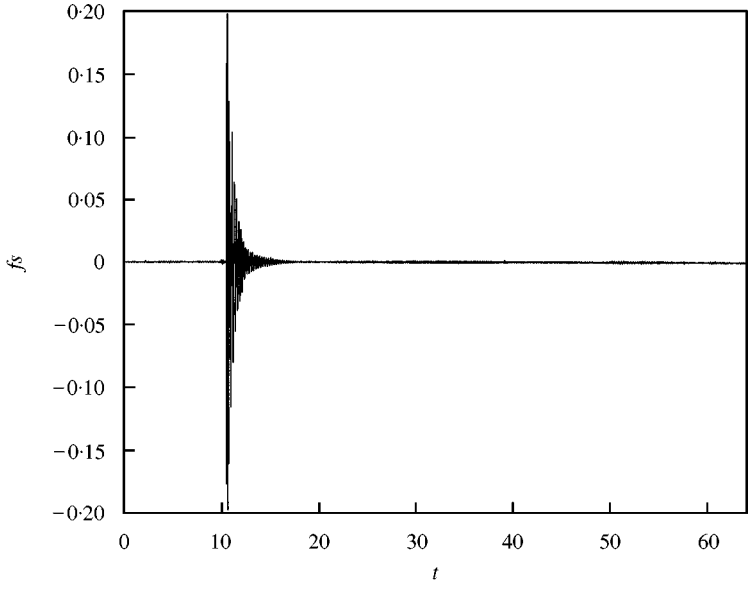

Figure 12. 8th floor original time-response to shock test (longitudinal direction).

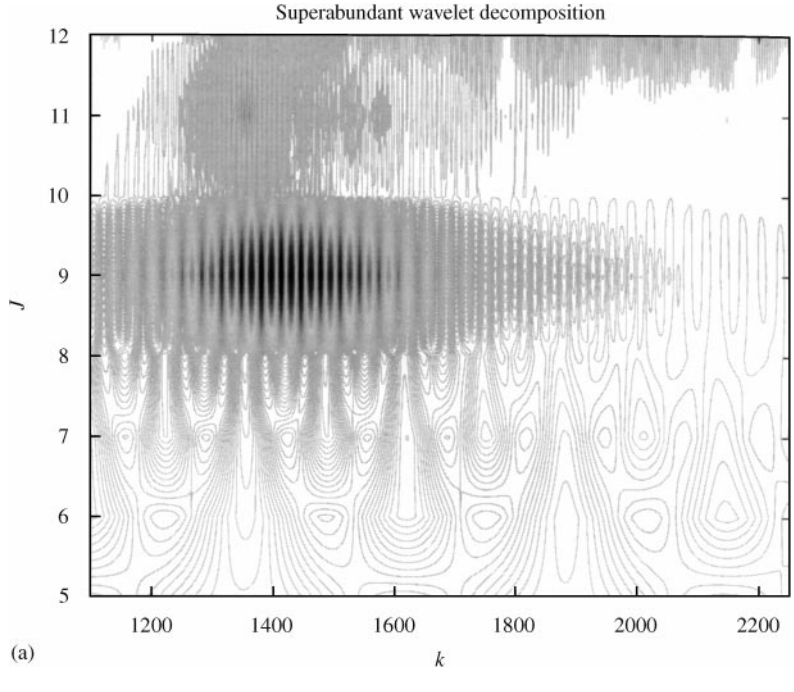

Figure 13. 8th floor longitudinal time-response to shock test. (a) Wavelet pyramidal decomposition in terms of translation parameters k and scales J. (b) Reconstruction of the first (scales $J = 8, 9$) and second (scale $J = 10$) modal responses. (c) Detail channels $(fd_J)_{J=5,\ldots,12}$. (d) Approximation channels $(fs_J)_{J=5,\ldots,13}$.

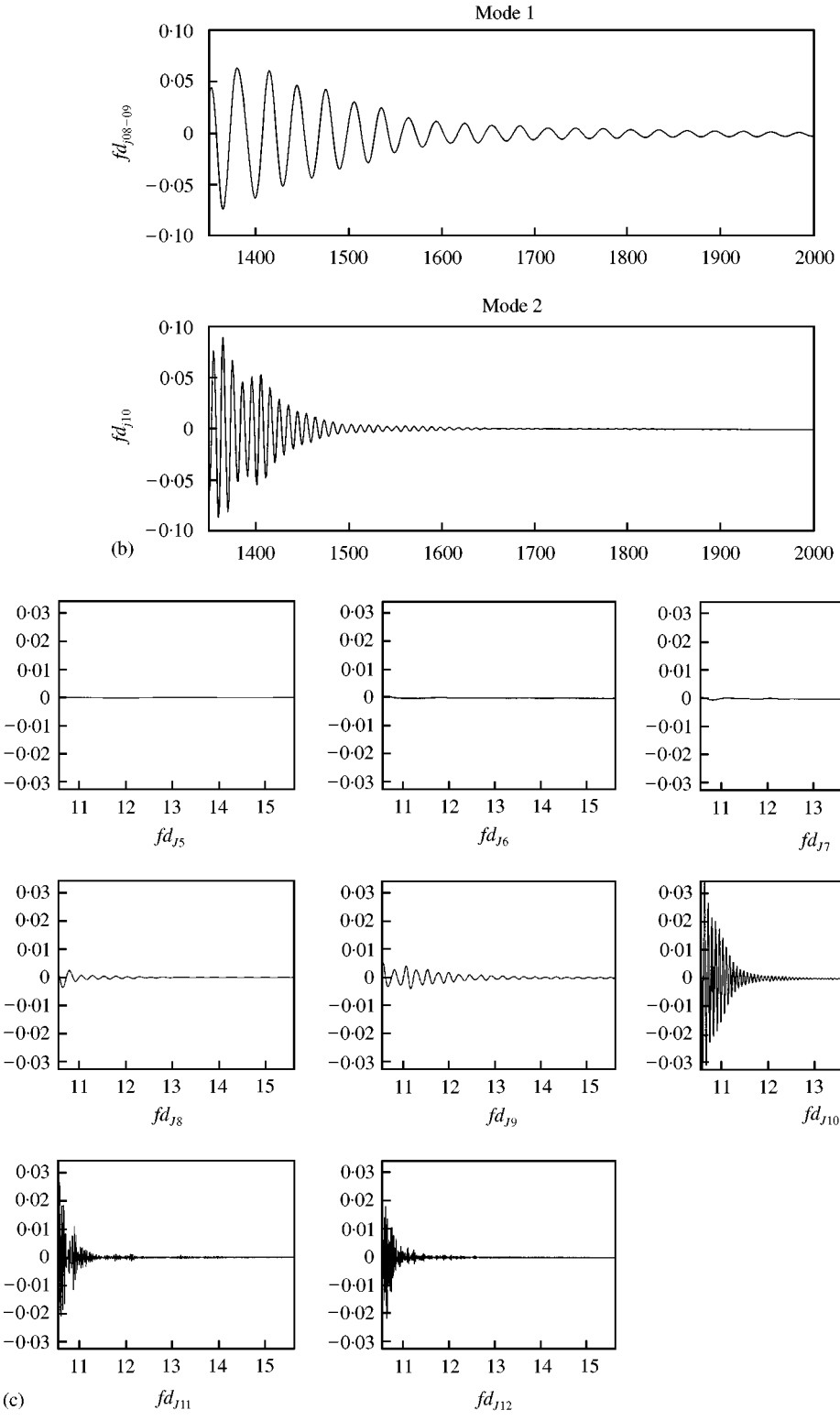

Figure 13. Continued.

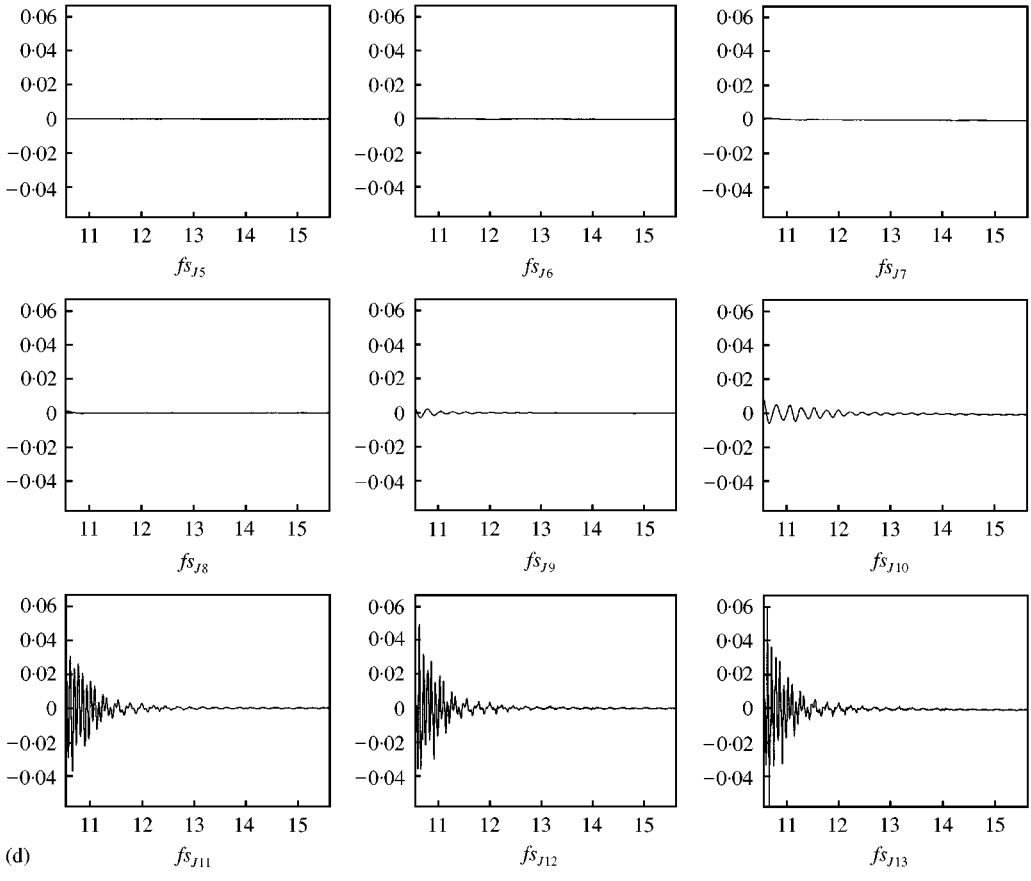

Figure 13. Continued.

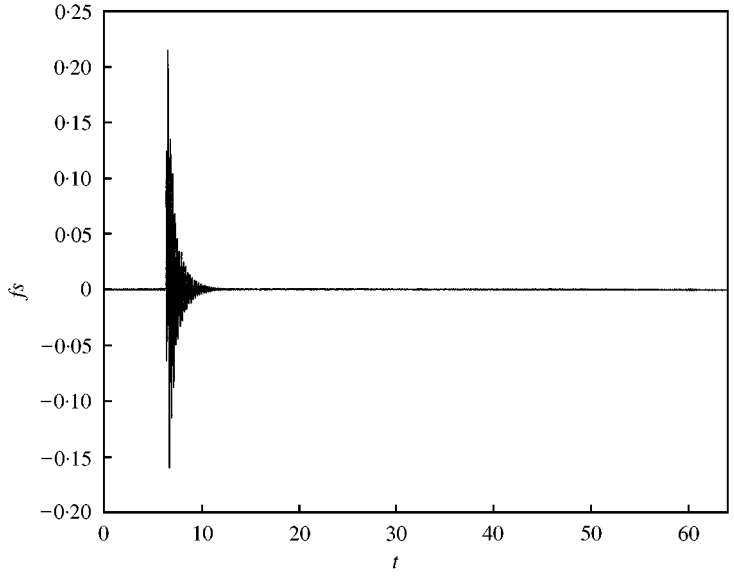

Figure 14. 8th floor original time-response to shock test (transverse direction).

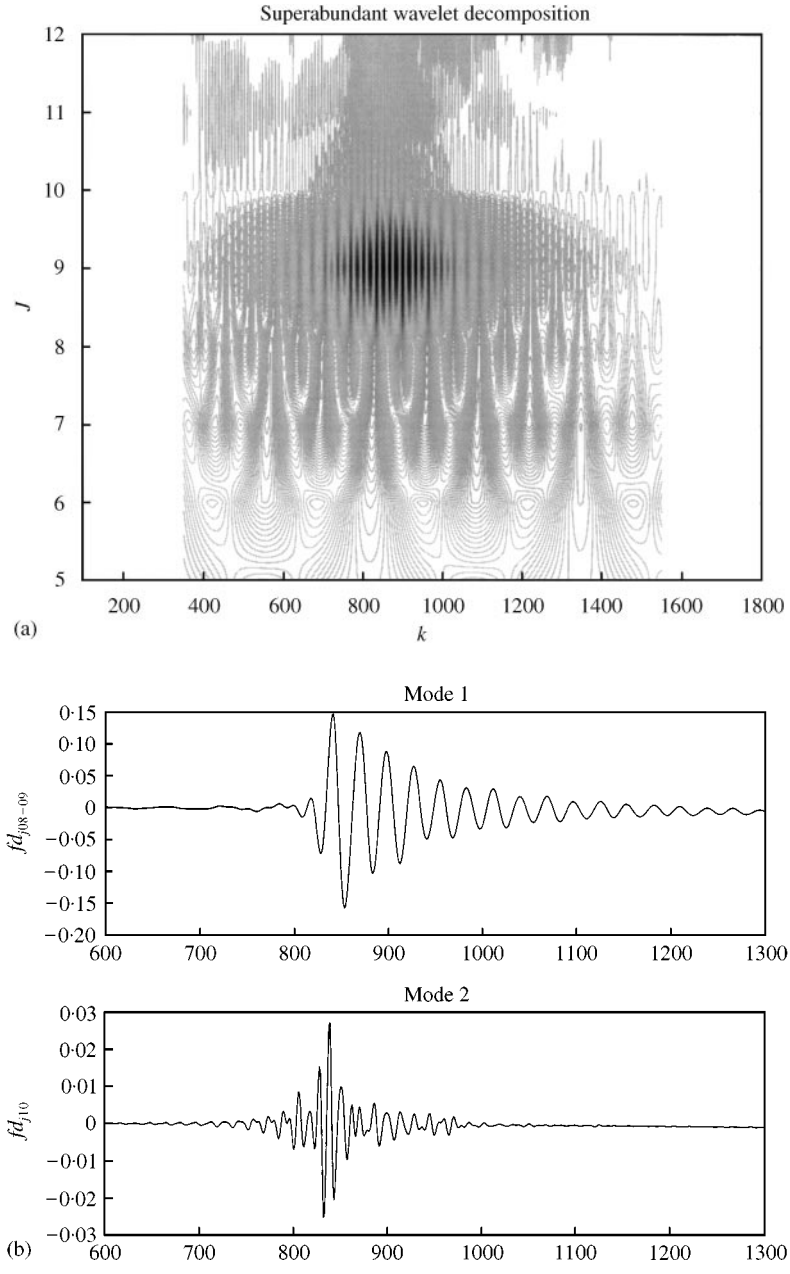

Figure 15. 8th floor transverse time-response to shock test. (a) Wavelet pyramidal decomposition in terms of translation parameters k and scales J. (b) Reconstruction of the first (scales $J = 8, 9$) and second (scale $J = 10$) modal responses. (c) Detail channels $(fd_J)_{J=5,\ldots,12}$. (d) Approximation channels $(fs_J)_{J=5,\ldots,13}$.

different eigenfrequency modes. If one is interested in identifying the damping using a standard superabundant analysis, formula (1) is applied with an accurate analyzing scale j_a to identify damping related to the first mode. The procedure is successively repeated with the higher modes by cutting-off channels related to the previous ones. A filtered counterpart may be implemented selecting specific channels to re-build a modal contribution as

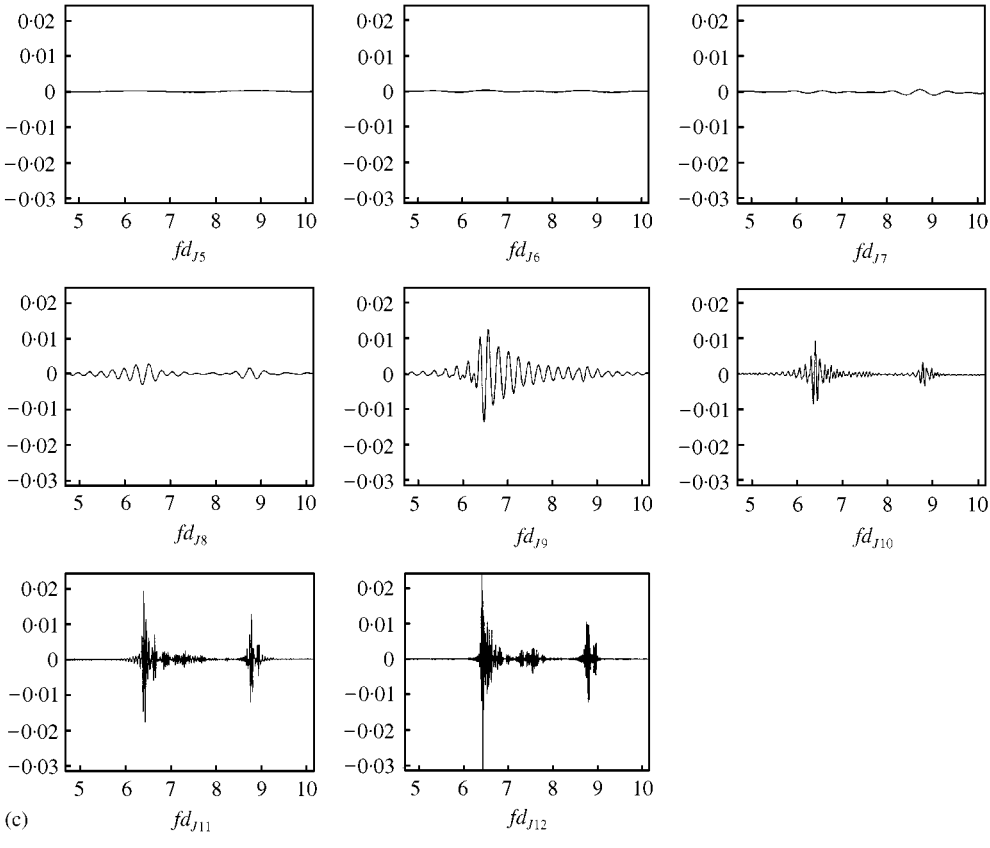

Figure 15. Continued.

depicted in Figures 9(b), 11(b), 13(b) and 15(b). Successive detail and approximation channels such as those in Figures 9(c) and 9(d), and 11(c) and 11(d), 13(c) and 13(d) and 15(c) and 15(d) are useful to set the time-window parameters required by the wavelet-logarithmic formula to locate the coefficients extrema.

In the case of harmonic excitation, the first (resp. second) modal contribution is extracted from the signal response using detail channels $J = 9, 10$ (resp. $J = 11$) whereas in the case of a shock excitation, the first and second modes are, respectively, related to detail channels $J = 8$, 9, and 10, whatever the direction is. It is noticeable that the harmonic testing procedure is weakly exciting the second mode as pointed out in Figures 9(b), 11(b), 13(b) and 15(b) and consequently cannot permit a damping estimate of the second mode.

4.2. NUMERICAL RESULTS

Dynamic properties of the first and second eigenfrequency modes computed using either the standard wavelet formula or a logarithmic decrement associated with a wavelet pre-filtering or still a filtered wavelet-logarithmic formula are gathered in Tables 2–7. Damping estimates produced from experimental data emphasize that the wavelet-based damping identification technique is relevant with well-correlated results. Simulations demonstrate that damping estimates sensitively depend on the acceleration level: for

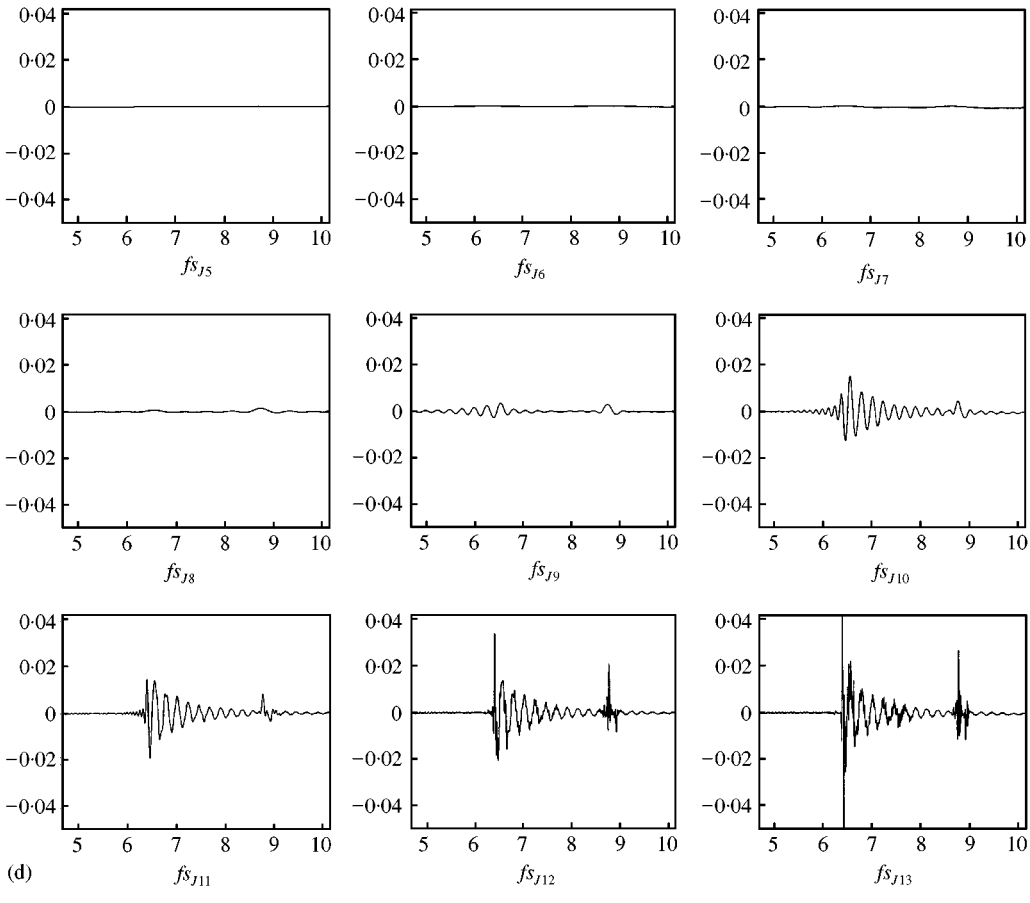

Figure 15. Continued.

instance, Tables 2 and 4 highlight first mode damping values of $0{\cdot}031 \pm 0{\cdot}002$ for a harmonic excitation to be compared with $0{\cdot}028 + 0{\cdot}001$ for a shock excitation. Still, it is noticeable that magnitude orders remain the same.

5. CONCLUSION

Part 2 of the paper was dedicated to an experimental application of the wavelet-logarithmic decrement formula theoretically established in reference [5] using *in situ* dynamic time-responses of a civil engineering building loaded with both harmonic and shock excitations. Simulations demonstrate that wavelet tools permit to uncouple the eigenfrequency modes of a m.d.o.f. system and to identify associated dampings. Damping estimates appear to be relevant with magnitude orders that remain stable. Using standard identification techniques, damping estimates are often perturbed by important errors related to multi-modal contributions, non-linear effects or excitation defaults for instances: here, damping estimates computed with the wavelet-logarithmic decrement are accurate with magnitude orders that remain stable. Time-scale representations such as the ones depicted in Figures 9(a)–15(a) also appear to be very useful to localize eigenfrequency

TABLE 2

Non-dimensional damping ratio of the building's fundamental mode excited in the longitudinal direction with a harmonic wave

Estimated non-dimensional damping ratio ξ							
Mode		Fundamental mode (Mode 1)			Frequency	4·2 Hz	
Direction		Longitudinal			Excitation	Harmonic wave	
Sampling frequency		128 Hz			Finest scale	$J = 13$	
Significant scales		Extract channels: $j \in \{9, 10\}$			Analyzing scale	$J_a = 11$	
IDENTIFICATION METHOD		Sensor no 1 (Level 8)	Sensor no 2 (Level 6)	Sensor no 3 (Level 4)	Sensor no 4 (Level 1)	Mean value	Standard deviation
Wavelet decrement	ξ	0·0282	0·0310	0·0305	0·0387	0·0308	0·0020
Filtered logarithmic decrement	ξ	0·0397	0·0300	0·0291	0·0315	0·0308	0·0023
Filtered wavelet decrement	ξ	0·0364	0·0304	0·0291	0·0326	0·0315	0·0014

TABLE 3

Non-dimensional damping ratio of the building's fundamental mode excited in the tranverse direction with a harmonic wave

Estimated non-dimensional damping ratio ξ							
Mode		Fundamental mode (Mode 1)			Frequency	4·57 Hz	
Direction		Transverse			Excitation	Harmonic wave	
Sampling frequency		128 Hz			Finest scale	$J = 13$	
Significant scales		Extract channels: $j \in \{9, 10\}$			Analyzing scale	$J_a = 11$	
IDENTIFICATION METHOD		Sensor no 1 (Level 8)	Sensor no 2 (Level 6)	Sensor no 3 (Level 4)	Sensor no 4 (Level 1)	Mean value	Standard deviation
Wavelet decrement	ξ	0·0340	0·0329	0·0319	0·0349	0·0334	0·0005
Filtered logarithmic decrement	ξ	0·0337	0·0363	0·0361	0·0364	0·0362	0·0006
Filtered wavelet decrement	ξ	0·0323	0·0360	0·0360	0·0345	0·0353	0·0008

TABLE 4

Non-dimensional damping ratio of the building's fundamental mode excited in the longitudinal direction with a shock

Estimated non-dimensional damping ratio ξ							
Mode Direction Sampling frequency Significant scales		Fundamental mode (Mode 1) Longitudinal 128 Hz Extract channels: $j \in \{8, 9\}$			Frequency Excitation Finest scale Analyzing scale	4·25 Hz Shock test $J = 13$ $J_a = 10$	
IDENTIFICATION METHOD		Sensor no 1 (Level 8)	Sensor no 2 (Level 6)	Sensor no 3 (Level 4)	Sensor no 4 (Level 1)	Mean value	Standard deviation
Wavelet decrement	ξ	0·0282	0·0242	0·0288	0·0284	0·0285	0·0012
Filtered logarithmic decrement	ξ	0·0280	0·0270	0·0296	0·0306	0·0288	0·0008
Filtered wavelet decrement	ξ	0·0280	0·0270	0·0293	0·0309	0·0286	0·0008

TABLE 5

Non-dimensional damping ratio of the building's first harmonic mode excited in the longitudinal direction with a shock

Estimated non-dimensional damping ratio ξ							
Mode		1st harmonic mode (Mode 2)			Frequency	12·75 Hz	
Direction		Longitudinal			Excitation	Shock test	
Sampling frequency		128 Hz			Finest scale	$J = 13$	
Significant scales		Extract channels: $j \in \{10\}$			Analyzing scale	$J_a = 11$	
IDENTIFICATION METHOD		Sensor no 1 (Level 8)	Sensor no 2 (Level 6)	Sensor no 3 (Level 4)	Sensor no 4 (Level 1)	Mean value	Standard deviation
Filtered logarithmic decrement	ξ	0·0367	0·0393	0·0396	0·0402	0·0395	0·0007
Filtered wavelet decrement	ξ	0·0375	0·0388	0·0370	0·0399	0·0382	0·0005

TABLE 6

Non-dimensional damping ratio of the building's fundamental mode excited in the transverse direction with a shock

Estimated non-dimensional damping ratio ξ							
Mode		Fundamental mode (Mode 1)			Frequency	4·50 Hz	
Direction		Transverse			Excitation	Shock test	
Sampling frequency		128 Hz			Finest scale	$J = 13$	
Significant scales		Extract channels: $j \in \{8, 9\}$			Analyzing scale	$J_a = 10$	
IDENTIFICATION METHOD		Sensor no 1 (Level 8)	Sensor no 2 (Level 6)	Sensor no 3 (Level 4)	Sensor no 4 (Level 1)	Mean value	Standard deviation
Wavelet decrement	ξ	0·0396	0·0415	0·0431	0·0396	0·0405	0·0007
Filtered logarithmic decrement	ξ	0·0336	0·0362	0·0370	0·0394	0·0366	0·0010
Filtered wavelet decrement	ξ	0·0336	0·0356	0·0364	0·0381	0·0360	0·0008

TABLE 7

Non-dimensional damping ratio of the building's fundamental mode excited in the transverse direction with a shock

Estimated non-dimensional damping ratio ξ							
Mode		1st harmonic mode (Mode 2)			Frequency	15·7 Hz	
Direction		Transverse			Excitation	Shock test	
Sampling frequency		128 Hz			Finest scale	$J = 13$	
Significant scales		Extract channels: $j \in \{10\}$			Analyzing scale	$J_a = 11$	
IDENTIFICATION METHOD		Sensor no 1 (Level 8)	Sensor no 2 (Level 6)	Sensor no 3 (Level 4)	Sensor no 4 (Level 1)	Mean value	Standard deviation
Filtered logarithmic decrement	ξ	0·0634	0·0559	0·0468	0·0576	0·0568	0·0030
Filtered wavelet decrement	ξ	0·0624	0·0357	0·0397	0·0339	0·0377	0·0062

modes. The latter two statements highlight the relevance of the wavelet procedure. Future prospects will now focus on the wavelet analysis of dynamic systems using a frequency domain approach.

REFERENCES

1. M. ZACEK 1996 *Construire parasismique*: *risque parasismique*, *conception parasismique des bâtiments*, *réglementation*. Marseille: Editions parenthèses.
2. C. BOUTIN and S. HANS 1997 *International Conference on Engineering Mechanics Today Hanoi*, *HCM City*, *August* 10. Contrôle du comportement de bâtiments par mesures de vibrations.
3. C. BOUTIN and S. HANS 1998 *Eleventh European Conference on Earthquake Engineering*. Paris, *September* 1998, 12. Using buildings to be demolished for vulnerability assessment.
4. C. BOUTIN, E. IBRAIM and S. HANS *Auscultation de bâtiments réels en vue de l'estimation de la vulnérabilité*. 5^{eme} *Colloque National AFPS*99, 298–305. Génie parasismique et réponse dynamique des ouvrages.
5. C. H. LAMARQUE, S. PERNOT and A. CUER 2000 *Journal of Sound and Vibration* **235**, 361–374. Damping identification in MDOF systems via a wavelet-logarithmic decrement—Part 1: Theory.
6. I. R. STUBBS and V. R. MACLAMORE 1973 *Fifth World Conference On Earthquake Engineering*, *Rome*, *Italy*. The ambient vibration survey.
7. M. N. FARSI 1996 *Thèse de Doctorat*, *Université Joseph Fourier*, *Grenoble*. Identification des structures de Génie Civil à partir de leur réponse vibratoire, vulnérabilité du bâti existant.
8. J. PAQUET 1976 *Annales de ITBTP* **200**, 129–151. Etude expérimentale du comportement dynamique des structures.
9. R. E. ENGLEKIRK and R. B. MATTHIESEN 1967 *Bulletin of the Seismological Society of America* **57**, 421–436. Forced vibration of an eight-story reinforced concrete building.
10. P. C. JENNINGS and J. H. KUROIWA 1968 *Bulletin of the Seismological Society of America* **58**, 891–916. Vibration and soil structure interaction tests of a nine-story reinforced concrete building.
11. J. PETROWSKI, D. JURUKOVSKI and T. PASKALOV 1973 *Fifth World Conference on Earthquake Engineering*, *Rome*, *Italy*. Dynamic properties of fourteen-story reinforced concrete building from full-scale vibration study and formulation of mathematical model.